CMLS, Cell. Mol. Life Sci. 54 (1998) 148–151
1420-682X/98/020148-04 $ 1.50 + 0.20/0

CMLS Cellular and Molecular Life Sciences

Relationship between steady-state activation and availability of cardiac sodium channel: evidence of uncoupling

V. A. Maltsev and A. I. Undrovinas*

Department of Medicine, Division of Cardiovascular Medicine, Henry Ford Heart Heart and Vascular Institute, Education & Research Building, 2799 West Grand Boulevard, Detroit (Michigan 48202-2689, USA), Fax +1 313 876 03001

Received 1 October 1997; received after revision 28 October 1997; accepted 13 November 1997

Abstract. The coupling between steady-state activation and availability from inactivation was characterized for the cardiac Na^+ channel. To evaluate this coupling, we plotted the relationship between the conductance and availability curve midpoint potentials measured in 92 rat ventricular cardiomyocytes and applied a correlation analysis. We found a high correlation between the midpoints (correlation coefficient = 0.86, slope = 0.95) within the availability midpoint potential range positive to −100 mV. In contrast, the midpoints were not correlated in the myocytes (37 of 92 cells) having midpoint potential negative to −100 mV, indicating an uncoupling between activation and availability.

Key words. Sodium current availability and activation; patch clamp; rat ventricular cardiomyocytes.

Voltage-sensitive Na^+ channels are responsible for the initial rapid increase in membrane permeability to Na^+, which is essential for the generation and propagation of cardiac action potential. However, not all Na^+ channels participate in cell excitation. In different cardiomyocytes, from about 90 to 50% of the channels are already inactivated at the resting potential [1–5]. The Na^+ channel availability curve (A–V) has a sigmoidal shape that desribes the fraction of channels which are available for excitation at a given membrane voltage, particularly at the resting potential. Another important factor determining the number of Na^+ channels participating in cell excitation is the threshold voltage at which channels begin to open. The threshold voltage is directly related to the position of the voltage-dependent steady-state activation curve (G–V). Accordingly, the actual number of Na^+ channels recruited for membrane depolarization upon excitation at a given resting potential is determined by the interplay of the positions of the A–V and G–V curves. From this point of view, an important question arises as to whether all cardiomyocytes have identical steady-state activation and availability and if not, what the activation-availability relationship is. Available data on this relationship are limited and contradictory. The midpoints reported in the literature for cardiac Na^+ channels vary widely for both activation (from −70 to −30 mV) and availability (from −120 to −70 mV). This diversity was attributed to differences among species, experimental protocols and recording conditions. One major obstacle to measuring the parameters is a spontaneous shift of activation and availability that occurs for cardiac Na^+ channels in while-cell configuration [2] as well as in cell-free and cell-attached patches [3]. In perfused canine cardiac Purkinje cells, the shift occurred almost equally for both activation and availability [2]. In contrast, a significantly smaller spontaneous shift for activation as compared with availability was reported for rat ventricular cardiomyocytes [4] and expressed human cardiac channel [5], indicating that the parameters might be uncoupled. How-

* Corresponding author.

ever, the relationship between steady-state activation and availability has not yet been systematically investigated. The goal of the present study was to clarify the relationship for Na^+ current in ventricular cardiomyocytes. To minimize spontaneous time-dependent shifts of the parameters, the steady-state activation and availability were determined shortly after establishment of the recording configuration.

Materials and methods

Isolation of cardiomyocytes. Ventricular cardiomyocytes were enzymatically isolated from Sprague-Dawley rat hearts into Ca^{2+}-free minimum essential medium with 10 mM HEPES (pH 7.3 with KOH) as previously described [6]. After isolation, cells were kept at 22 °C in the same solution supplied with 0.3 mM $CaCl_2$.

Whole-cell current recordings. Whole-cell recordings of the Na^+ current (I_{Na}) were made at 22–24 °C by the patch-clamp technique [7] in rat ventricular cardiomyocytes. The pipettes, made of borosilicate glass capillaries, had a tip resistance of 0.6 to 0.8 MΩ in standard solutions. Ion currents were recorded by an Axopatch 200A patch-clamp amplifier (Axon Instruments, Foster City, CA, USA). The maximum deviation (V_{dev}) from voltage command associated with series resistance (R_s) was estimated as $V_{dev} = I_{max} R_s$. In all experiments non-compensated R_s was less than 2 MΩ. Electronic series resistance compensation (K_s) was imposed to a point just before oscillations occurred. The final setting of K_s value (on the Axopatch 200A amplifier) varied from 75 to 95%. The maximum I_{Na} values (I_{max}) varied from 5 to 30 nA, so that with R_s compensation, V_{dev} was estimated as $V_{dev} = I_{max} R_s (100\% - K_s)/100\%$. Satisfactory voltage control was assumed if $V_{dev} < 2$ mV, and only these cells were included in the study. Currents were filtered at 10 kHz (−3 dB) using a four-pole low-pass Bessel filter and then digitized at a 50-kHz sampling rate using a DigiData 1200 interface and pClamp 6.0 software (Axon Instruments). The curve fittings were performed by StatMost v.2.50 sotware (DataMost, Salt Lake City, UT, USA). Solutions for whole-cell experiments were selected to suppress all currents other than I_{Na}. The external bath solution was composed of (in mM): NaCl 10, CsCl 125, $CaCl_2$ 1, $MgCl_2$ 1.2, glucose 11 and HEPES 20 (pH 7.4 with CsOH). The internal pipette solution was composed of (in mM): NaCl 10, CsF 115, CsCl 20, MgATP 2.5, EGTA 5.0 and HEPES 5.0, pH (7.3 with CsOH). All chemicals were purchased from Sigma (USA).

Voltage clamp protocols. Steady-state voltage-dependent availability (A–V) from inactivation was determined using a series of 1-s-long conditioning steps to various membrane potentials (V) followed by a test depolarization of 18 ms duration to −30 mV to assess the pool of available Na^+ channels. A 980-ms interval, at a holding potential of −170 mV, separated the individual pulse protocols and allowed for full recovery of I_{Na}. Steady-state activation relationships (G–V) were obtained from transformations of the peak current (I_{peak})–voltage relationships. The I_{peak} values were measured in response to a series (0.5 Hz) of test depolarizations to various potentials from a holding potential of −150 mV.

Data analysis. To determine A–V curves, I_{peak} values were normalized to the maximum I_{peak} value and plotted against the conditioning potential V. The data points were then fitted to a Boltzmann function:

$$A = \{1 + \exp[(V - V_{\frac{1}{2}A})/K_A]\}^{-1},$$

where $V_{\frac{1}{2}A}$ is the midpoint of the relationship, and K_A is a slope factor. The maximum Na^+ conductance (g_{max}) and reversal potential (V_{rev}) were estimated from a linear fit (as the slope and intercept with the voltage axis, respectively) of an almost linear ascending portion of the (I_{peak})-voltage relationship in the range from −25 mV to 0 mV. The Na^+ conductance (g) at each test potential (V_t) was calculated as

$$g = I_{peak}/(V_t - V_{rev}).$$

The data points of normalized conductance ($G = g/g_{max}$) were fitted to a Boltzmann function:

$$G = \{1 + \exp[(V_{\frac{1}{2}G} - V_t)/K_G]\}^{-1},$$

where $V_{\frac{1}{2}G}$ is the midpoint of the relationship and K_G is a slope factor.

To minimize time-dependent shifts of G–V and A–V curves, we determined the parameters in each cell within 3 min after establishment of whole-cell configuration. The evaluated systematic error in our determinations related to the time-dependent parameter shift of the midpoint potentials was less than 1 mV, since the initial shift rate was 0.254 ± 0.043 mV/min and 0.296 ± 0.023 mV/min, for $V_{\frac{1}{2}G}$ and $V_{\frac{1}{2}A}$, respectively ($n = 51$). All results are presented as the mean ± SD of independent determinations.

Results

The mean values of $V_{\frac{1}{2}G}$ and $V_{\frac{1}{2}A}$ were -54.61 ± 7.11 mV and -97.13 ± 9.96 mV ($n = 92$), respectively. The parameter values varied in a wide range; minimum and maximum values for $V_{\frac{1}{2}G}$ were −65.12 mV and −33.45 mV, and for $V_{\frac{1}{2}A}$ −113.8 mV and −72.8 mV, respectively. The distributions of both $V_{\frac{1}{2}G}$ and $V_{\frac{1}{2}A}$ were asymmetrical and displayed a steep decline toward negative values (fig. 1A, B) but different decline of steepness toward positive potentials. In contrast, the distributions of the slope factors (K_G and K_A) were almost symmetrical and easily fitted by a Gaussian function (fig. 1C, D). The K_G and K_A values did not

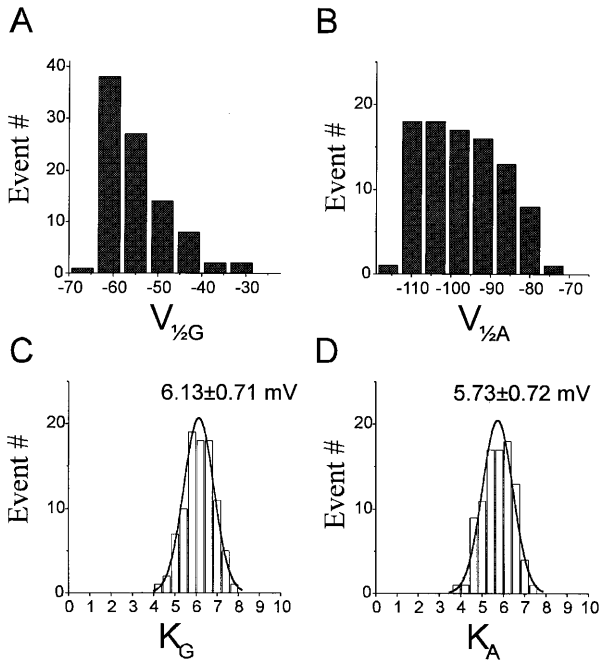

Figure 1. Distribution of the parameters of steady-state activation (*A*, *C*) and availability (*B*, *D*). Asymmetrical distribution for the midpoint potentials for activation, $V_{\frac{1}{2}G}$ (*A*), and availability, $V_{\frac{1}{2}A}$ (*B*). Symmetrical distributions of the slope factors for activation, K_G (*C*), and availability, K_A (*D*). Solid lines represent Gaussian fit to the histograms (means $\pm$ SD are shown at the curves). Bin size for the histrograms was 0.4 mV. Data were collected from 92 myocytes.

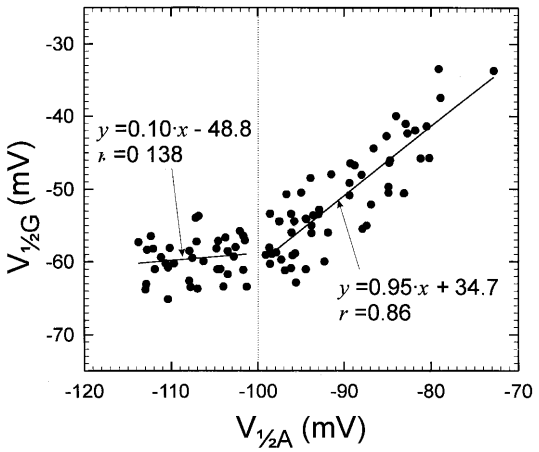

Figure 2. Relationship between the midpoints of steady-state activation ($V_{\frac{1}{2}G}$) and availability ($V_{\frac{1}{2}A}$). The closed circles represent data points measured in 92 myocytes. The data were analysed separately for two $V_{\frac{1}{2}A}$ ranges: $V_{\frac{1}{2}A} < -100$ mV and $V_{\frac{1}{2}A} > -100$ mV (separated by a dotted line in the plot). Indicated are results of linear regression (arrows) with equation (y) and correlation coefficient (r) for both $V_{\frac{1}{2}A}$ regions.

correlate with each other, and no correlation was found between the slope factors and the respective midpoint values (not shown).

The entire $V_{\frac{1}{2}G}-V_{\frac{1}{2}A}$ relationship (fig. 2) was nonlinear. However, in the $V_{\frac{1}{2}A}$ range positive to -100 mV (shown by a dotted line in fig. 2), the cell-to-cell variations of $V_{\frac{1}{2}}$ and $V_{\frac{1}{2}G}$ were well coupled with a correlation coefficient and a slope of linear regression close to 1. In contrast, no correlation was found between $V_{\frac{1}{2}G}$ and $V_{\frac{1}{2}A}$ in a population of myocytes (40%, 37 of 92 cells) that had $V_{\frac{1}{2}A}$ values negative to -100 mV. In this $V_{1/2A}$ range, the correlation coefficient and the slope of the relationship were close to zero.

Discussion

The absence of a correlation between $V_{\frac{1}{2}G}$ and $V_{\frac{1}{2}G}$ found in the present study in the cell population with $V_{\frac{1}{2}A} < -100$ mV suggests an uncoupling between availability and activation. The differences between our results and a previous report of a linear $V_{\frac{1}{2}G}-V_{\frac{1}{2}A}$ relation [2] can be explained by the fact that previous studies did not compare the midpoint potentials but only their relative changes during spontaneous time-dependent shifts. Different temperature conditions between the two studies might also explain the discrepancy. On the other hand, our data are in line with the previous single-channel studies. In fact, a smaller shift in the activation process compared with availability was observed for canine cardiac Na^+ channels in cell-free and cell-attached patches [3]. This appears to be an important characteristic of the cardiac Na^+ channel, since the differene in the shifts was documented for cardiac isoforms of Na^+ channel but not for skeletal muscle [5].

A possible mechanism for the $V_{\frac{1}{2}A}-V_{\frac{1}{2}G}$ variations could be related to different gating modes of Na^+ channels. The midpoint potentials were found to be different for 'fast' ($V_{\frac{1}{2}A} = -90$ mV, $V_{\frac{1}{2}G} = -48$ mV) and 'slow' ($V_{\frac{1}{2}A} = -70$ mV, $V_{\frac{1}{2}G} = -61$ mV) gating modes [8], assuming an opposite slope of the $V_{\frac{1}{2}G}-V_{\frac{1}{2}A}$ relationship compared with that reported here (fig. 2) or elsewhere [2]. Furthermore, the distribution for K_A values showed only one dominant peak with a mean value close to 6 mV (fig. 1D), whereas the 'slow inactivation mode' was characterized by a dramatic increase in the availability slope factor (up to 13 mV). Thus, modal channel behaviour does not explain the $V_{\frac{1}{2}A}-V_{\frac{1}{2}G}$ variations shown in the present study.

It has been recently shown that, in addition to the primary channel structure [5, 9, 10], other factors such as state of channel phosphorylation [11] and the channel environement, including membrane phosopholipid composition and the membrane-attached cytoskeleton [4, 6, 12], are involved in Na^+ channel gating. The latter might be relevant to the cell-to-cell variations of the steady-state activation and availability found in the present study. For example, F-actin disruption alters single Na^+ channel inactivation without changes in activation [6]. In addition, F-actin-based cytoskeleton modulates availability curve shifts by about 20 mV, whereas activation shifts could be modulated by micro-

tubular cytoskeleton by 12 mV [4]. A different position of the availability curve in myocytes might indicate an intrinsic mechanism regulating cell excitation. In fact, the $V_{\frac{1}{2}G}$ value reflects a threshold of the myocyte excitation. From this point of view, the limit for $V_{\frac{1}{2}G}$ variations found in the present study ($V_{\frac{1}{2}G} > -65$ mV, see figs 1, 2) may have physiological importance in maintaining the threshold for cell excitation that prevents premature excitations.

The strong $V_{\frac{1}{2}G}-V_{\frac{1}{2}A}$ coupling found in the $V_{\frac{1}{2}A}$ voltage range positive to -100 mV (fig. 2) may also be important in the regulation of cell excitation. Indeed, cells with a more positive $V_{\frac{1}{2}A}$ will have a higher channel availability at a fixed resting potential. At the same time, a relatively more positive $V_{\frac{1}{2}G}$ value will inevitably cause the myocyte to be more resistant to activation because of a higher excitation threshold, thus preventing premature discharges. In the case of more negative $V_{\frac{1}{2}A}$ values, reflecting a lesser number of available channels, a concomitant change of $V_{\frac{1}{2}G}$ in the same negative direction will result in threshold reduction and, thus, facilitate the excitation.

Two populations of cells with different availability-activation coupling found in the present study may imply functional heterogeneity of ventricular myocytes. Heterogeneity of the myocytes within the ventricular wall has been previously documented, particularly with respect to the shape of the action potential and the density of functional K^+ channels [13, 14]. We speculate that the apparent availability-activation uncoupling for Na^+ channels found in the present study may produce a dispersion of myocyte excitability and excitation propagation velocity within the myocardium to optimize functional performance of different myocardial regions.

Acknowledgements. Our appreciation is extended to B. Malleis and N. Undrovinas for their assistance in single cardiomyocyte preparation. We thank Dr. H. N. Sabbah for critical reading of the manuscript. The study was supported in part by a grant from the National Heart, Lung and Blood Institute HL53819.

1 Wendt D. J., Starmer C. F. and Grant A. O. (1992) Na channel kinetics remain stable during perforated-patch recordings. Am. J. Physiol. **263:** C1234–C1240
2 Hanck D. A. and Sheets M. F. (1992) Time-dependent changes in kinetics of Na^+ current in single canine cardiac Purkinje cells. Am. J. Physiol. **262:** H1197–H1207
3 Berman M. F., Camardo J. S., Robinson R. B. and Siegelbaum S. A. (1989) Single sodium channels from canine ventricular myocytes: voltage dependence and relative rates of activation and inactivation. J. Physiol. (Lond.) **415:** 503–531
4 Maltsev V. A. and Undrovinas A. I. (1997) Cytoskeleton modulates coupling between availability and activation of cardiac sodium channel. Am. J. Physiol. **273:** H1832–H1840
5 Wang D. W., George A. L. and Bennett P. B. (1996) Comparison of heterologously expressed human cardiac and skeletal muscle sodium channels. Biophys. J. **70:** 283–245
6 Undrovinas A. I., Shander G. S. and Makielski J. C. (1995) Cytoskeleton modulates gating of voltage-dependent sodium channel in heart. Am. J. Physiol. **269:** H203–H214
7 Hammil O. P., Marty A., Neher E., Sakmann B. and Sigworth J. (1981) Improved patch-clamp techniques for high-resolution current recording from cells and cell-free membrane patches. Pflugers Arch. **391:** 85–100
8 Böhle T., Biskup C., Koopmann R. and Benndorf K. (1997) Steady state inactivation and steady state activation in different gating modes of Na^+ channel action. Biophys. J. (Abstract) **72:** A116
9 Chahine M., George A. L. Jr, Zhou M., Ji S., Sun W., Barchi R. L. et al. (1994) Sodium channel mutations in paramyotonia congenita uncouple inactivation from activation. Neuron **12:** 281–294
10 West J. W., Patton D. E., Scheuder T., Wang A. L., Goldin Y. and Catterall W. A. (1992) A cluster of hydrophobic amino acid residues required for fast Na^+-channel inactivation. Proc. Natl. Acad. Sci. USA **89:** 10910–10914
11 Sunami A., Fan Z., Nakamura F., Naka M., Tanaka T., Sawanobori T. et al. (1991) The catalytic subunit of cyclic AMP-dependent protein kinase directly inhibits sodium channel activities in guinea-pig ventricular myocytes. Pflugers Arch. **419:** 415–417
12 Undrovinas A. I., Fleidervish I. A. and Makielski J. C. (1992) Inward sodium current at resting potentials in single cardiac myocytes induced by the ischemic metabolite lysophosphatidylcholine. Circ. Res. **71:** 1231–1241
13 Antzelevitch C., Sicouri S., Litovsky S. H., Lukas A., Krishnan S. C., Di Diego J. M. et al. (1991) Heterogeneity within the ventricular wall. Electrophysiology and pharmacology of epicardial, endocardial and M cells. Circ. Res. **69**: 1427–1449
14 Gintant G. A. (1995) Regional differences in I_K density in canine left ventricle: role of $I_{K,s}$ in electrical heterogeneity. Am. J. Physiol. **268:** H604–H613